JHEP

Published for SISSA by Springer

Received: November 28, 2022
Revised: March 10, 2023
Accepted: June 17, 2023
Published: June 29, 2023

# Measurement of the branching fraction of $J/\psi \to \rho\pi$ at KEDR

## The KEDR collaboration

V.V. Anashin,[a] O.V. Anchugov,[a] A.V. Andrianov,[a] K.V. Astrelina,[a] V.M. Aulchenko,[a,b] E.M. Baldin,[a,b] G.N. Baranov,[a,c] A.K. Barladyan,[a] A.Yu. Barnyakov,[a,b,c] M.Yu. Barnyakov,[a,b,c] I.Yu. Basok,[a] A.M. Batrakov,[a] E.A. Bekhtenev,[a] O.V. Belikov,[a] D.E. Berkaev,[a] A.E. Blinov,[a,b] V.E. Blinov,[a,b,c] M.F. Blinov,[a] A.V. Bobrov,[a,b] V.S. Bobrovnikov,[a,b] A.V. Bogomyagkov,[a,b] D.Yu. Bolkhovityanov,[a] A.E. Bondar,[a,b] A.R. Buzykaev,[a,b] P.B. Cheblakov,[a,b] V.L. Dorohov,[a,c] F.A. Emanov,[a] V.V. Gambaryan,[a] D.N. Grigoriev,[a,b,c] V.V. Kaminskiy,[a] S.E. Karnaev,[a] G.V. Karpov,[a] S.V. Karpov,[a] K.Yu. Karukina,[a,c] D.P. Kashtankin,[a] P.V. Kasyanenko,[a] A.A. Katcin,[a] T.A. Kharlamova,[a] V.A. Kiselev,[a] S.A. Kononov,[a,b] A.A. Krasnov,[a] E.A. Kravchenko,[a,b] V.N. Kudryavtsev,[a,b] V.F. Kulikov,[a,b] I.A. Kuyanov,[a] E.B. Levichev,[a,c] P.V. Logachev,[a] D.A. Maksimov,[a,b] Yu.I. Maltseva,[a] V.M. Malyshev,[a] A.L. Maslennikov,[a,b] O.I. Meshkov,[a,b] S.I. Mishnev,[a] I.A. Morozov,[a] I.I. Morozov,[a,b] D.A. Nikiforov,[a] S.A. Nikitin,[a] I.B. Nikolaev,[a,b] I.N. Okunev,[a] S.B. Oreshkin,[a] A.A. Osipov,[a,b] I.V. Ovtin,[a,c] A.V. Pavlenko,[a] S.V. Peleganchuk,[a,b] P.A. Piminov,[a] N.A. Podgornov,[a] V.G. Prisekin,[a,b] O.L. Rezanova,[a,b] A.A. Ruban,[a,b] G.A. Savinov,[a] A.G. Shamov,[a,b] L.I. Shekhtman,[a] D.A. Shvedov,[a] B.A. Shwartz,[a,b] E.A. Simonov,[a] S.V. Sinyatkin,[a] A.N. Skrinsky,[a] A.V. Sokolov,[a,b] E.V. Starostina,[a,b] D.P. Sukhanov,[a] A.M. Sukharev,[a,b] A.A. Talyshev,[a,b] V.A. Tayursky,[a,b] V.I. Telnov,[a,b] Yu.A. Tikhonov,[a,b] K.Yu. Todyshev,[a,b,1] A.G. Tribendis,[a] G.M. Tumaikin,[a] Yu.V. Usov,[a] A.I. Vorobiov,[a] V.N. Zhilich,[a,b] A.A. Zhukov,[a] V.V. Zhulanov[a,b] and A.N. Zhuravlev[a,b]

[a] *Budker Institute of Nuclear Physics, SB RAS, Novosibirsk 630090, Russia*
[b] *Novosibirsk State University, Novosibirsk 630090, Russia*
[c] *Novosibirsk State Technical University, Novosibirsk 630092, Russia*

*E-mail:* todyshev@inp.nsk.su

[1] Corresponding author



https://doi.org/10.1007/JHEP06(2023)196

JHEP06(2023)196

Abstract: We present the study of the decay $J/\psi \to \rho\pi$. The results are based on of 5.2 million $J/\psi$ events collected by the KEDR detector at the VEPP-4M collider. The branching fractions are measured to be $\mathcal{B}(J/\psi \to \rho\pi) = (2.072 \pm 0.017 \pm 0.062) \cdot 10^{-2}$ and $\mathcal{B}(J/\psi \to \pi^+\pi^-\pi^0) = (1.878 \pm 0.013 \pm 0.051) \cdot 10^{-2}$, where the first uncertainties are statistical and the second systematic. Our results are more precise than the previous relative measurements.

Keywords: $e^+$-$e^-$ Experiments, Particle and Resonance Production, Quarkonium

ArXiv ePrint: 2211.13520

JHEP06(2023)196

## Contents



## 1 Introduction

In this paper, a study for $J/\psi$ meson decays of the type $J/\psi \to \rho\pi$ is presented. All three decay modes $J/\psi \to \rho^+\pi^-, J/\psi \to \rho^-\pi^+$ and $J/\psi \to \rho^0\pi^0$ are examined.

The probability of the $J/\psi \to \rho\pi$ decay is the largest among hadronic $J/\psi$ decays with an intermediate resonance and is $\mathcal{B}(J/\psi \to \rho\pi) = (1.69 \pm 0.15)\%$ [1]. Nine experiments contributed to the $J/\psi \to \rho\pi$ branching fraction measurement [2–10]. At the moment, there is a noticeable discrepancy between the results of early experiments [2–8] and the latest measurements by collaborations BES [9] and BaBar [10]. The Particle Data Group (PDG) gives the value of the scale factor 2.4. This motivates us to perform new measurement of the $J/\psi \to \rho\pi$ branching fraction. The decay $J/\psi \to \rho\pi$ is the main process leading to the final three-pion state, the study of which is important in itself. The branching fraction of the process $J/\psi \to \pi^+\pi^-\pi^0$ have been measured directly by the MARKII [6], BES [9, 11] and BaBar [12, 13] collaborations.

In addition to the circumstances already indicated, the study of decays into three $\pi$ mesons is important for a better understanding of the rescattering effects, which, for example, are discussed in refs. [14, 15]. Refinement of the $J/\psi \to \rho\pi$ branching fraction will be useful in the study of the so-called $\rho-\pi$ puzzle [6]. It would also be interesting to compare the value of this branching fraction with a relatively recent theoretical calculation given in ref. [16].



JHEP06(2023)196

We also note that the exact determination of the $J/\psi \to \rho\pi$ branching fraction may be important in the analysis of other processes for which the decay considered in this article is a background process.

## 2 Theoretical framework and MC simulation

The differential cross section of the process $J/\psi \to \pi^+\pi^-\pi^0$ can be written as a sum of contributions of several intermediate states $\rho(770)\pi$, $\rho(1450)\pi$, $\omega\pi$, $\rho(1700)\pi$. In this paper, we consider the first two terms, which are dominant. We neglect the remaining terms as well as contribution of the decay $J/\psi \to \pi^+\pi^-\pi^0$ without intermediate resonances, the corresponding systematic errors are considered in section 4.1. Under these conditions, the expression for the differential cross section has the form

$$\frac{d\sigma}{d\Gamma} \propto \left|\sum_j a_j + \sum_j b_j e^{i\phi}\right|^2 = \left|\sum_j a_j\right|^2 + \left|\sum_j b_j\right|^2 + \sum_{i,j}\left(a_i b_j^* e^{-i\phi} + a_i^* b_j e^{i\phi}\right), \tag{2.1}$$

where $d\Gamma$ is a phase space element, $j$ can be $0, +, -$ corresponding to the charged states $\rho(770)$ and $\rho(1450)$. The amplitudes $a_j$ and $b_j$ are the functions of $s$ and pions momenta and correspond to neutral and charged modes of $\rho(770)$ and $\rho(1450)$ resonances. The amplitude for neutral mode can be written as

$$a_0 = a_{\rho^0\pi^0} = (\mathbf{p}_+ \times \mathbf{p}_-)\sin\theta_n \frac{m_{\rho^0}^2}{q^2 - m_{\rho^0}^2 + iq\Gamma_{\rho^0}(q^2)} \sqrt{\mathcal{B}(J/\psi \to \rho^0\pi^0)\mathcal{B}(\rho^0 \to \pi^+\pi^-)}, \tag{2.2}$$

where $\mathbf{p}_+$ and $\mathbf{p}_-$ are charged pion momenta, $\theta_n$ is an angle between the normal to the reaction plane and the beam axis, $\Gamma_{\rho^0}(q^2) = \Gamma_{\rho^0}\left(\frac{p_\pi(q^2)}{p_\pi(m_{\rho^0}^2)}\right)^3\left(\frac{m_{\rho^0}^2}{q^2}\right)$, $m_{\rho^0}$ and $\Gamma_{\rho^0}$ are the mass and the width of the $\rho^0(770)$, $q$ is the invariant mass of the pion pair, $p_\pi$ is the pion momentum in the $\rho$ rest frame. The amplitude $b_0$ is written in the same way by replacing the $\rho(770)$ to $\rho(1450)$. The above parametrization goes back to the work of G.J. Gounaris and J.J. Sakurai [17].

Consider, for example, one of the terms in the last sum of the expression (2.1)

$$\begin{aligned}
&a_0 b_0^* e^{-i\phi} + a_0^* b_0 e^{i\phi} \\
&= \sqrt{\mathcal{B}(J/\psi \to \rho^0\pi^0)\mathcal{B}(\rho^0 \to \pi^+\pi^-)}\sqrt{\mathcal{B}(J/\psi \to \rho^0(1450)\pi^0)\mathcal{B}(\rho^0(1450) \to \pi^+\pi^-)} \\
&\quad \times (\mathbf{p}_+ \times \mathbf{p}_-)^2 \sin^2\theta_n \\
&\quad \times \left[\frac{2m_{\rho^0}^2 m_{\rho^0(1450)}^2 (q^4 + m_{\rho^0}^2 m_{\rho^0(1450)}^2 + q^2\Gamma_{\rho^0}\Gamma_{\rho^0(1450)})}{((q^2 - m_{\rho^0}^2)^2 + q^2\Gamma_{\rho^0}^2)((q^2 - m_{\rho^0(1450)}^2)^2 + q^2\Gamma_{\rho^0(1450)}^2)}\cos\phi\right. \\
&\quad - \frac{2m_{\rho^0}^2 m_{\rho^0(1450)}^2 q^2 (m_{\rho^0}^2 + m_{\rho^0(1450)}^2)}{((q^2 - m_{\rho^0}^2)^2 + q^2\Gamma_{\rho^0}^2)((q^2 - m_{\rho^0(1450)}^2)^2 + q^2\Gamma_{\rho^0(1450)}^2)}\cos\phi \\
&\quad + \frac{2m_{\rho^0}^2 m_{\rho^0(1450)}^2 (q^3\Gamma_{\rho^0(1450)} + q\Gamma_{\rho^0} m_{\rho^0(1450)}^2)}{((q^2 - m_{\rho^0}^2)^2 + q^2\Gamma_{\rho^0}^2)((q^2 - m_{\rho^0(1450)}^2)^2 + q^2\Gamma_{\rho^0(1450)}^2)}\sin\phi \\
&\quad \left. - \frac{2m_{\rho^0}^2 m_{\rho^0(1450)}^2 (q^3\Gamma_{\rho^0} + q\Gamma_{\rho^0(1450)} m_{\rho^0(1450)}^2)}{((q^2 - m_{\rho^0}^2)^2 + q^2\Gamma_{\rho^0}^2)((q^2 - m_{\rho^0(1450)}^2)^2 + q^2\Gamma_{\rho^0(1450)}^2)}\sin\phi\right]
\end{aligned} \tag{2.3}$$

The other cross terms in (2.1) can be obtained by appropriate replacement of the indices in (2.3). One can represent this expression as a sum of $(c^+_{00} - c^-_{00}) \cdot \cos\phi + (d^+_{00} - d^-_{00}) \cdot \sin\phi$, where c and d are the corresponding terms in formula (2.3). Then expression (2.1) can be rewritten as a sum

$$\frac{d\sigma}{d\Gamma} = A + B + C^+ \cos\phi - C^- \cos\phi + D^+ \sin\phi - D^- \sin\phi, \tag{2.4}$$

where $A = \left|\sum_j a_j\right|^2$, $B = \left|\sum_j b_j\right|^2$, $C^\pm = \sum_{i,j} c^\pm_{ij}$, and $D^\pm = \sum_{i,j} d^\pm_{ij}$. To calculate detection efficiency, we should simulate separately six contributions entering in (2.4).

Similarly, we considered the possible interference of the $J/\psi \to \rho\pi$ process with a nonresonant decay into three pions, $J/\psi \to \omega\pi$ and $J/\psi \to \rho(1700)\pi$. This is discussed in section 4.1. The signal MC samples of all contributions are generated for the analysis.

It should be noted that the exact expressions for the amplitudes contain constants that are not essential in the MC simulation, but which are important in determining the coupling constants. The corresponding ratios are as follows [18]: $|g_{J/\psi\gamma}| = \left[\frac{3m^3_{J/\psi}\Gamma_{J/\psi}\mathcal{B}(J/\psi\to e^+e^-)}{4\pi\alpha}\right]^{\frac{1}{2}}$, $|g_{J/\psi\rho\pi}| = \left[\frac{4\pi\Gamma_{J/\psi}\mathcal{B}(J/\psi\to\rho\pi)}{W(m_{J/\psi})}\right]^{\frac{1}{2}}$, where $W(s)$ is a phase space factor, $\Gamma_{J/\psi}$ is total $J/\psi$ width, $\mathcal{B}(J/\psi \to e^+e^-)$ and $\mathcal{B}(J/\psi \to \rho\pi)$ are branching fractions for the mentioned decays.

The KEDR simulation program is based on the GEANT package, version 3.21 [19]. The $J/\psi$ decays were simulated with the BES generator [20] based on the JETSET 7.4 code [21] and tuned in the KEDR experiment [22]. That allowed us to determine accurately the number of $J/\psi$ events to obtain the desired branching fractions. The BHWIDE [23] and MCGPJ generators [24] provided simulation of $e^+e^- \to e^+e^-\gamma$ and $e^+e^- \to \mu^+\mu^-\gamma$ events to define the background from dileptonic processes. To determine hadronic background, we simulated the exclusive processes $J/\psi \to K^0_S K^*(892)^0, K^*(892)^+K^- + c.c.$ with kaons and decay of $J/\psi$ into vector-pseudoscalar $J/\psi \to \rho\eta, \rho\eta', \phi\eta, \omega\eta, \omega\pi^0$ using generators of the KEDR simulation package.

## 3 Experiment and data analysis

The data sample used in this analysis was taken by the KEDR detector [25] at the VEPP-4M collider [26]. The process was analysed for a 1.4 pb$^{-1}$ data accumulated at the $J/\psi$ peak consisting of about $5.23 \cdot 10^6$ resonance decays.

### 3.1 Event selection

We select $J/\psi \to \rho\pi$ events by applying criteria on the track multiplicity and event topology. Two reconstructed tracks are required to have $d < 3$ cm and $|z_0| < 17$ cm, where $d$ is the track impact parameter relative to the beam axis and $z_0$ is the coordinate of the closest approach point. Only events with at least one track from interaction region ($d < 0.75$ cm,$|z_0| < 13$ cm) or two tracks with $d < 0.75$ cm were accepted. We also required two clusters in the calorimeter not associated to tracks ("neutral clusters") with energies



JHEP06(2023)196

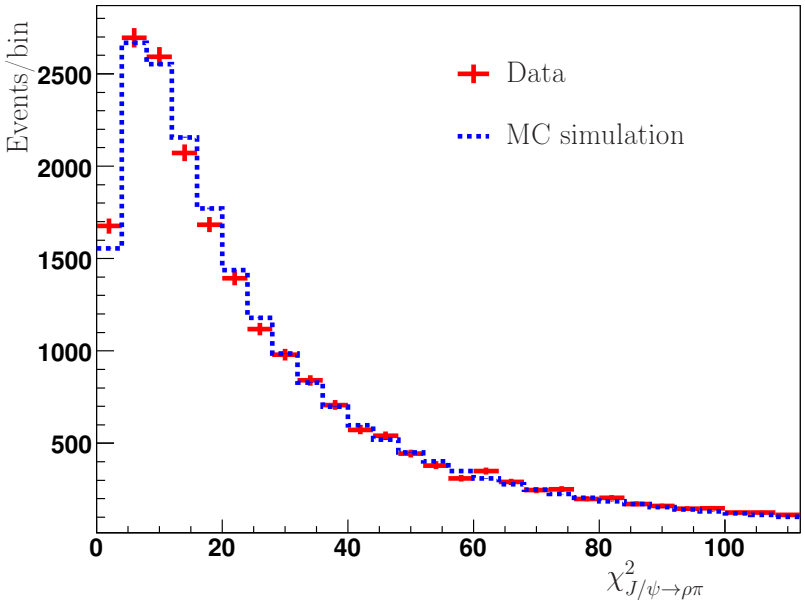


**Figure 1**. $\chi^2$ distribution of kinematic fit for $J/\psi \to \rho\pi$ selected candidate events.

exceeding $E_1 = 50\,\text{MeV}$ or one cluster with an energy greater than $E_2 = 150\,\text{MeV}$. The selected events are fitted kinematically. A kinematic fit is applied to reconstruct the candidate events for two hypotheses: $J/\psi$ decay into $\pi^+\pi^-\pi^0$ and $J/\psi$ decay to $K^+K^-\pi^0$ in final state. Neutral pion is reconstructed either from two neutral clusters, otherwise from one neutral cluster ("merged" $\pi^0$) with energy greater than $E_2$. The kinematic fit adjusts the cluster energy and the track momentum within the measured uncertainties so as to satisfy energy and momentum conservation for the given event hypothesis. In the case of the merged photons the momentum conservation condition was not required. In further selection of events, $\chi^2_{\pi^+\pi^-\pi^0}$ from a kinematic fit must be less than 90 and also satisfy the condition $\chi^2_{\pi^+\pi^-\pi^0} < \chi^2_{K^+K^-\pi^0}$. Figure 1 shows the $\chi^2$ distribution of the kinematic fits for the selected $J/\psi \to \rho\pi$ events.

The subsequent stages of the analysis were carried out in accordance with the ref. [27]. Three subsets of events are selected according to the following conditions: $\cos\theta_{\pi^+\pi^0} > \cos\theta_{\pi^+\pi^-} \ \wedge \ \cos\theta_{\pi^+\pi^0} > \cos\theta_{\pi^-\pi^0}$, $\cos\theta_{\pi^-\pi^0} > \cos\theta_{\pi^+\pi^-} \ \wedge \ \cos\theta_{\pi^-\pi^0} > \cos\theta_{\pi^+\pi^0}$, and $\cos\theta_{\pi^+\pi^-} > \cos\theta_{\pi^-\pi^0} \ \wedge \ \cos\theta_{\pi^+\pi^-} > \cos\theta_{\pi^+\pi^0}$. Here and below, $\theta_{\pi^+\pi^0}$, $\theta_{\pi^+\pi^-}$ and $\theta_{\pi^+\pi^-}$ are the angles between the momentum vectors of the corresponding $\pi$ mesons. Figure 2 shows the experimental distribution of these cosines.

For the suppression of the background induced by the processes $e^+e^-(\gamma)$, $\mu^+\mu^-(\gamma)$ for events with "merged" $\pi^0$ we used the additional criteria. The ratio of Fox-Wolfram moments [28] $H_2/H_0$ was required to be less than 0.8. The ratio of the energy deposited in the calorimeter to the measured momentum of the charged particle $E/p$ must be less than 0.75. The sum $\cos\theta_{\pi^+\pi^-} + \cos\theta_{\pi^+\pi^0} + \cos\theta_{\pi^-\pi^0}$ was required to be less than $-1.075$, this distribution lies in the range of $-1.5$ to $-1$.



JHEP06(2023)196

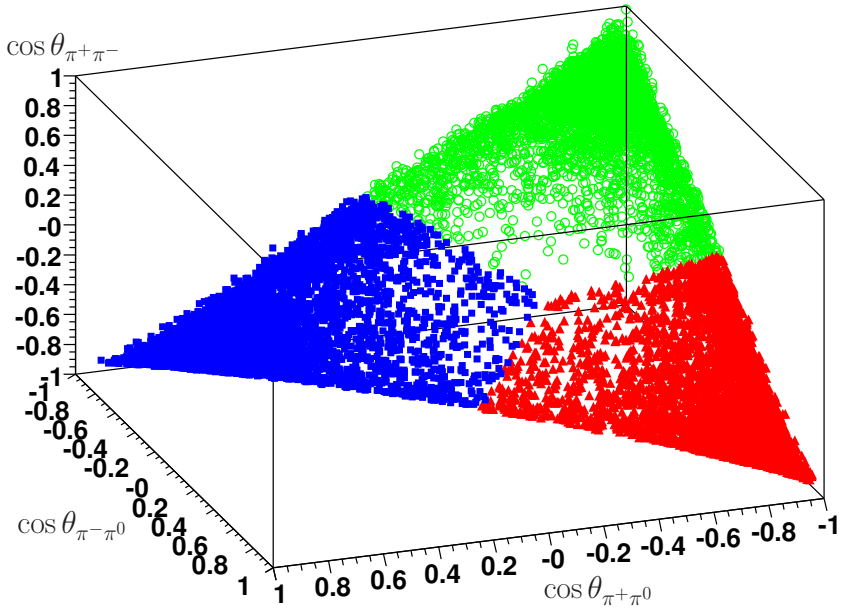


**Figure 2**. The experimental distribution of events over the cosines $\cos\theta_{\pi^+\pi^0}, \cos\theta_{\pi^-\pi^0}, \cos\theta_{\pi^+\pi^-}$. Triangle, square and circle markers correspond to the conditions that single out the $J/\psi$ meson decays to $\rho^+\pi^-$, $\rho^-\pi^+$ and $\rho^0\pi^0$, respectively.

To reduce events with neutral clusters overlapped from those associated with track, we also required $\cos\theta_{\pi^+\pi^-} > -0.95$ for events considered as $J/\psi \to \rho^+\pi^-$ and $J/\psi \to \rho^-\pi^+$ decays.

### 3.2 Analysis procedure

In our analysis, we perform a binned simultaneous fit of the $\rho^0$, $\rho^+$ and $\rho^-$ invariant mass distributions. The bin sizes are chosen equal to $24\,\mathrm{MeV}/c^2$ for the neutral decay mode and $22\,\mathrm{MeV}/c^2$ for the charged decay modes. The expected number of events as function of the $\rho$ invariant mass for given decay mode is parameterized as follows:

$$\begin{aligned} n^{\mathrm{theor}}(q) = \mathcal{B}_{\rho\to\pi\pi}\mathcal{B}_{\pi^0\to\gamma\gamma}\Big[ & p_1\epsilon_1 H_{\rho\pi} + \epsilon_2 p_2 H_{\rho(1450)\pi} \\ & + (\epsilon_3 H^{c+}_{\rho\pi,\rho(1450)\pi} - \epsilon_4 H^{c-}_{\rho\pi,\rho(1450)\pi})\cos\phi\sqrt{p_1p_2} \\ & + (\epsilon_5 H^{s+}_{\rho\pi,\rho(1450)\pi} - \epsilon_6 H^{s-}_{\rho\pi,\rho(1450)\pi})\sin\phi\sqrt{p_1p_2}\Big] + \sum \epsilon_{\mathrm{bkgs}} H_{\mathrm{bkgs}}, \end{aligned} \tag{3.1}$$

where $p_1$ and $p_2$ are parameters related to decays probabilities and $\phi$ is the interference phase. They are free in the fit. $H_{\rho\pi}$, $H_{\rho(1450)\pi}$, $H^{c\pm}_{\rho\pi,\rho(1450)\pi}$ and $H^{s\pm}_{\rho\pi,\rho(1450)\pi}$ are the distributions corresponding to the terms A, B, C and D in (2.4). These distributions are proportional to the integrals of the functions $A$, $B$, $C^\pm$ and $D^\pm$ over the phase space and initially normalized to $N_{\mathrm{sig}} - N_{\mathrm{bkgs}}$, where $N_{\mathrm{sig}}$ is the number of selected events of the given $J/\psi \to \rho\pi$ decay mode and $N_{\mathrm{bkgs}}$ is the expected number of background events. The detection efficiencies $\epsilon_i$ and $\epsilon_{\mathrm{bkgs}}$ are obtained from the MC simulation.



JHEP06(2023)196

| Decay channel | Modes of the decay $J/\psi \to \rho\pi$ | | |
|---|---|---|---|
| | $\rho^0\pi^0$ | $\rho^+\pi^-$ | $\rho^-\pi^+$ |
| Contribution $e^+e^- \to e^+e^-(\gamma), \mu^+\mu^-(\gamma)$ | | | |
| | $0.2 \pm 0.1$ | $0.7 \pm 0.1$ | $0.8 \pm 0.1$ |
| Hadronic contributions | | | |
| $K^0_S K^*(892)^0 + c.c.$ | $0.4 \pm 0.1$ | – | – |
| $K^+ K^*(892)^-$ | – | $0.5 \pm 0.1$ | – |
| $K^- K^*(892)^+$ | – | – | $0.5 \pm 0.1$ |

**Table 1**. Background contributions to the fit are listed in percent.

For the $J/\psi \to \rho^0\pi^0$ decay, the main hadronic background arises from $J/\psi \to K^0_S K^*(892)^0 \to K^0_S K^+\pi^- + c.c.$ decays, while for the $J/\psi \to \rho^+\pi^-$ and $J/\psi \to \rho^-\pi^+$ the dominated part of the hadronic contamination is due to decays $J/\psi \to K^+K^*(892)^- \to K^+K^0_S\pi^-$ and $J/\psi \to K^-K^*(892)^+ \to K^-K^0_S\pi^+$, respectively. These contributions, as well as the possible contributions of the QED processes $e^+e^- \to e^+e^-(\gamma)$, $e^+e^- \to \mu^+\mu^-(\gamma)$ were simulated and included into the last term of the fitting function (3.1). All of them are given in table 1. The expected number of background events was estimated using the total number $J/\psi$ decays, branching fractions of the background processes and their detection efficiencies.

We introduce raw branching fraction $\mathcal{B}^{\rm sig}_{\rm raw} = N_{\rm sig}/(\epsilon_1 N_{J/\psi})$, where $N_{J/\psi}$ is the number of $J/\psi$ events determined with the equation $N_{J/\psi} = N^{\rm sel}_{\rm hadr}/\epsilon_{J/\psi}$, $N^{\rm sel}_{\rm hadr}$ is the number of the selected hadronic $J/\psi$ decays. The $J/\psi$ detection efficiency $\epsilon_{J/\psi}$ is derived from the MC simulation. The product of $p_1$ by $\mathcal{B}^{\rm sig}_{\rm raw}$ allows one to determine the branching fraction of the decay $J/\psi \to \rho\pi$ using selected $J/\psi \to \rho\pi$ events $\mathcal{B}^{\rm sig} = p_1 \cdot \mathcal{B}^{\rm sig}_{\rm raw}$. For the branching fraction $\mathcal{B}_{\rho\to\pi\pi}$ one has $\mathcal{B}_{\rho^0\to\pi^+\pi^-} = 0.98906 \pm 0.0016, \mathcal{B}_{\rho^\pm\to\pi^\pm\pi^0} = 0.99955 \pm 0.00005$ and $\mathcal{B}_{\pi^0\to\gamma\gamma} = 0.98823 \pm 0.00034$ PGD [1]. The described approach to fitting distributions was inspired by the article [29]. Note that this method differs from the Dalitz plot analysis, which is used, for example, in [30].

The observed number of signal events $N_{\rm sig}$, expected number of background events $N_{\rm bkgs}$ and related input quantities for all individual decay modes are summarized in table 2.

The numbers of $J/\psi \to \rho\pi$ events observed at each decay modes $j$ and each invariant mass interval $k$ were fitted simultaneously as a function of invariant mass using a minimizing function

$$\chi^2 = \sum_j \sum_k \frac{(n^{\rm exp}_{jk} - n^{\rm theor}_{jk})^2}{n^{\rm exp}_{jk} + \sigma^2_{n^{\rm theor}_{jk}}} \tag{3.2}$$

where $n^{\rm exp}_{jk}$ and $n^{\rm theor}_{jk}$ are experimentally measured and theoretically calculated numbers of $J/\psi \to \rho\pi$ events, respectively. $\sigma_{n^{\rm theor}_{jk}}$ is error of the calculated $n^{\rm theor}_{jk}$.

Figure 3 shows the result of the fit of the $\rho$ meson's invariant mass distributions over all decay modes $J/\psi \to \rho^0\pi^0$, $J/\psi \to \rho^+\pi^-$ and $J/\psi \to \rho^-\pi^+$.

The fitting was carried out in the range of invariant masses up to $1.4\,{\rm GeV/c^2}$. The first three free parameters determine the branching fraction $\mathcal{B}(J/\psi \to \rho\pi)$ based on



JHEP06(2023)196

| Input quantity | Modes of the decay $J/\psi \to \rho\pi$ | | |
|---|---|---|---|
| | $J/\psi \to \rho^0\pi^0$ | $J/\psi \to \rho^+\pi^-$ | $J/\psi \to \rho^-\pi^+$ |
| $N_{\rm sig}$ | $5908 \pm 77$ | $6927 \pm 83$ | $6959 \pm 83$ |
| $N_{\rm bkgs}$ | $34.2 \pm 6.6$ | $77.6 \pm 9.9$ | $91.5 \pm 10.4$ |
| $\epsilon_1, \%$ | $6.32 \pm 0.01$ | $7.08 \pm 0.01$ | $7.18 \pm 0.01$ |
| $\epsilon_2, \%$ | $5.93 \pm 0.02$ | $8.39 \pm 0.02$ | $8.43 \pm 0.02$ |
| $\epsilon_3, \%$ | $6.17 \pm 0.02$ | $6.98 \pm 0.02$ | $7.09 \pm 0.02$ |
| $\epsilon_4, \%$ | $6.22 \pm 0.02$ | $6.97 \pm 0.02$ | $7.08 \pm 0.02$ |
| $\epsilon_5, \%$ | $6.22 \pm 0.02$ | $7.34 \pm 0.02$ | $7.43 \pm 0.02$ |
| $\epsilon_6, \%$ | $6.21 \pm 0.02$ | $7.11 \pm 0.02$ | $7.21 \pm 0.02$ |

**Table 2**. Summary of the signal and background yields, detection efficiencies for each decay mode. Statistical errors for values $N_{\rm sig}, \epsilon_{1...6}$ and total error for $N_{\rm bkgs}$ are indicated.

| $\mathcal{B}^+, \%$ | $\mathcal{B}^-, \%$ | $\mathcal{B}^0, \%$ | $\delta M$, MeV/c$^2$ | $\phi$, rad | $\chi^2/ndf$ | $P(\chi^2)$ |
|---|---|---|---|---|---|---|
| $2.028 \pm 0.029$ | $2.017 \pm 0.027$ | $2.053 \pm 0.030$ | $5.2 \pm 0.8$ | $-1.89 \pm 0.13$ | 122.2/121 | 0.45 |

**Table 3**. The main results of simultaneous fit (only statistical errors are presented).

subsets of events $J/\psi \to \rho^+\pi^-$, $J/\psi \to \rho^-\pi^+$ and $J/\psi \to \rho^0\pi^0$ modes. We will denote these parameters as $\mathcal{B}^+$, $\mathcal{B}^-$ and $\mathcal{B}^0$, respectively. The parameters defining the products $\mathcal{B}_{\rho^0(1450)\pi^0} \cdot \mathcal{B}(\rho(1450) \to \pi^+\pi^-)$, $\mathcal{B}_{\rho^+(1450)\pi^-} \cdot \mathcal{B}(\rho(1450) \to \pi^+\pi^0)$, $\mathcal{B}_{\rho^-(1450)\pi^+} \cdot \mathcal{B}(\rho(1450) \to \pi^-\pi^0)$ and the phase of the interference are also free, but we considered them as just auxiliary quantities. We took into account the possible shift of the invariant mass between experiment and simulation by introducing an additional free parameter $\delta M$. The function $n^{\rm theor}(q)$ is defined for all possible values of $q$, since a cubic spline approximation is constructed over the entire range of invariant masses. The branching fractions of the process $J/\psi \to \rho\pi$ obtained from the fit are presented in table 3.

Based on the fit results obtained, we determined the average value $\mathcal{B}(J/\psi \to \rho\pi) = (2.031 \pm 0.017) \cdot 10^{-2}$. This result is given without corrections, which are discussed in sections 4.1 and 4.5. Obtained similarly from the fitting results, the product $\mathcal{B}(J/\psi \to \rho(1450)\pi) \cdot \mathcal{B}(\rho(1450) \to \pi\pi)$ is equal to $(1.88 \pm 0.22) \cdot 10^{-4}$. At the same time, the contribution of the destructive interference of processes $J/\psi \to \rho\pi$ and $J/\psi \to \rho(1450)\pi$ to the observed cross section is approximately $-11.9\%$. The issue of determining the quantity $\mathcal{B}(J/\psi \to \rho(1450)\pi) \cdot \mathcal{B}(\rho(1450) \to \pi\pi)$ is described in more detail in section 5.

## 4 Discussion of systematic uncertainties in $\mathcal{B}(J/\psi \to \rho\pi)$

### 4.1 Systematic uncertainty of the fitting model

The inaccuracy of $\rho(1450)$ resonance parameters introduces uncertainty to the branching fraction obtained from the fit. This uncertainty is evaluated by the variation of the $\Gamma_{\rho(1450)}$



JHEP06(2023)196

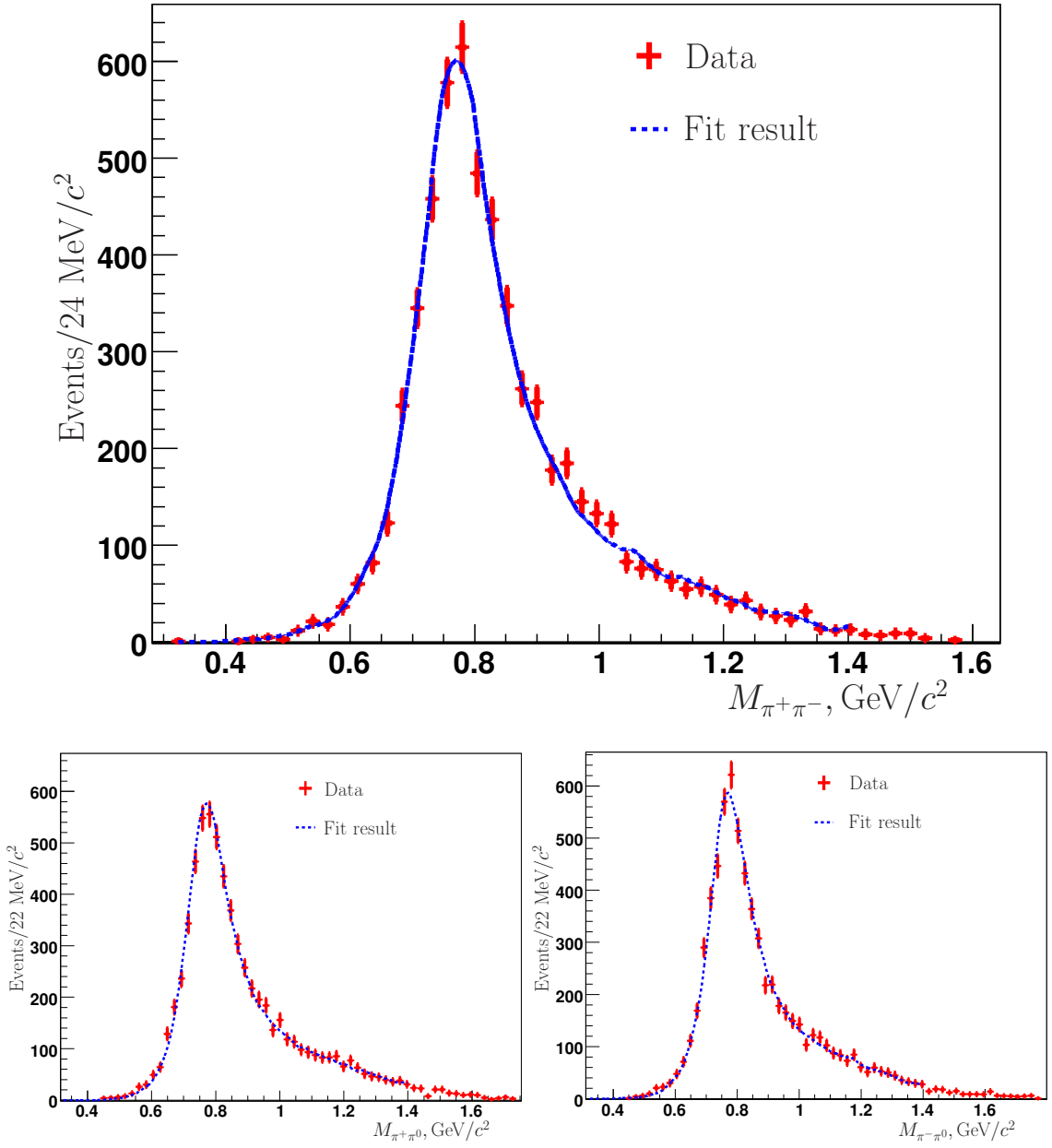


**Figure 3**. The invariant masses distributions of $\pi^+\pi^-$, $\pi^+\pi^0$ and $\pi^-\pi^0$. The dashed curve shows the result of the simultaneous fit. The experimental data set is presented in tables 10 and 11 in appendix.

and $M_{\rho(1450)}$ in the ranging of their errors 60 MeV and 25 MeV, respectively, taken from PDG [1]. The resulting changes of the $J/\psi \to \rho\pi$ branching fraction were 1.0% and 0.2%. The uncertainty related to the parameters of the $\rho(770)$ meson is due to an inaccuracy of 0.8 MeV in determining its total width [1] and is estimated at 0.5% in a similar way.

The possible contribution of the process $J/\psi \to \gamma f_2$ was simulated and included into the fit. The change of the measured branching fraction is $-0.2\%$. We apply this correction to the our result and include an additional 0.1% error into the systematic uncertainty.



JHEP06(2023)196

| Source | Uncertainty, % |
|---|---|
| Uncertainty $\Gamma_{\rho(1450)}$ | 1.0 |
| Uncertainty $M_{\rho(1450)}$ | 0.2 |
| Uncertainty $\Gamma_{\rho(770)}$ | 0.5 |
| Contribution of $\gamma f_2$ | 0.1 |
| Contribution $\rho(1700)\pi$ | 0.7 |
| Contribution $e^+e^- \to \pi^+\pi^-\pi^0$ | 0.6 |
| Contribution $\omega\pi$ | 0.2 |
| MC statistics | 0.2 |
| Uncertainties $\mathcal{B}_{\rho^0\to\pi^+\pi^-}$, $\mathcal{B}_{\rho^\pm\to\pi^\pm\pi^0}$, $\mathcal{B}_{\pi^0\to\gamma\gamma}$ | 0.1 |
| Sum in quadrature | 1.5 |

**Table 4**. The relative systematic uncertainties in $\mathcal{B}(J/\psi \to \rho\pi)$ due to approximation in the invariant mass distribution.

In equation (2.1), the contributions related to $J/\psi \to \omega\pi$, $J/\psi \to \rho(1700)\pi$ processes and nonresonant three-pion decay are omitted. The systematic uncertainties associated with this approximation were estimated by adding these terms one by one to equation (2.1) similarly to $J/\psi \to \rho(1450)\pi$ contribution as described in section 2. In each case two additional free parameters were introduced, the amplitude of the process and the interference phase.

The systematic uncertainties obtained are presented in table 4. We also took into account the MC statistical uncertainty and the systematic errors related to uncertainties in the $\mathcal{B}_{\rho^0\to\pi^+\pi^-}$, $\mathcal{B}_{\rho^\pm\to\pi^\pm\pi^0}$ and $\mathcal{B}_{\pi^0\to\gamma\gamma}$ parameters entering in (3.1).

### 4.2 Systematic uncertainty of the fitting procedure

Since we perform a simultaneous fitting of the $\rho$ meson's invariant mass distributions the results obtained are sensitive to the method of delimiting decay modes. To estimate this uncertainty we considered the alternative method of modes separation in accordance with the conditions $\cos\theta_{\pi^+\pi^-} < P \wedge \cos\theta_{\pi^+\pi^0} > \cos\theta_{\pi^-\pi^0}$, $\cos\theta_{\pi^+\pi^-} < P \wedge \cos\theta_{\pi^-\pi^0} > \cos\theta_{\pi^+\pi^0}$ and $\cos\theta_{\pi^+\pi^-} > P$ to select $J/\psi \to \rho^+\pi^-$, $J/\psi \to \rho^-\pi^+$ and $J/\psi \to \rho^0\pi^0$ events, respectively. The $P$ parameter varied from $-0.45$ to $-0.55$. We also modified the method described earlier by replacing "$\cos\theta_{\pi^+\pi^-}$" with "$\cos\theta_{\pi^+\pi^-} + \delta$" in all conditions listed in section 3.1. In our fit, we used the value of $\delta = -0.3$ according to ref. [27]. This value corresponds to the minimum intersection of the sets of events of the considered decay modes. The maximum change of the measured $J/\psi \to \rho\pi$ branching fraction for these two methods was 1.1%.

We have also varied the invariant mass ranges. When varying the upper invariant mass limit of the fit from $1.3\,\mathrm{GeV/c^2}$ to $1.8\,\mathrm{GeV/c^2}$, difference in the obtained $J/\psi \to \rho\pi$ branching fraction were less than 0.4%.

Systematic uncertainties described in this section are given in table 5.



JHEP06(2023)196

| Source | Uncertainty, % |
|---|---|
| Variation of the modes separation | 1.1 |
| Variation of the fit energy range | 0.4 |
| Sum in quadrature | 1.2 |

**Table 5**. The systematic uncertainties for $\mathcal{B}(J/\psi \to \rho\pi)$ associated with fitting procedure.

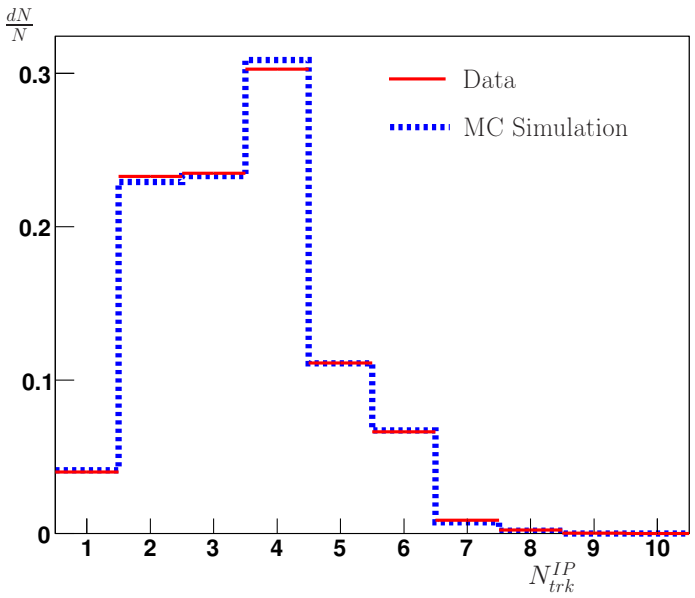


**Figure 4**. Distribution of the number of tracks from the interaction point at the $J/\psi$ peak. Distribution is normalized to unity.

### 4.3 Systematic uncertainty in the number of $J/\psi$ events

The details of the Monte-Carlo $J/\psi$ decay simulation and the procedure a reliable systematic uncertainty estimation are described in ref. [22]. Figure 4 shows comparison between $J/\psi \to hadrons$ data and the MC simulation for the distribution of the number of tracks from the interaction point. According to this work the error associated with the multihadron event $J/\psi$ generator is about 0.7%.

Taking into account the change in the condition of the detector compared to 2005, additional tuning of the $J/\psi$ decay simulation was carried out. As a result, the detection efficiency of the multihadron events changed by 0.4%.

In addition, we varied criteria for the hadron selection to evaluate the effect of other possible sources of a systematic uncertainty. The sum in quadrature of all errors obtained by the variation of the selection criteria is about 0.8%.

Summing up in quadratures these three values, we obtain that the conservative error in determining the branching fraction due to the uncertainty in the number of $J/\psi$ decays is 1.1%.



JHEP06(2023)196

| Source | Uncertainty, % |
|---|---|
| Track reconstruction | 0.5 |
| $\pi^0$ reconstruction | 0.2 |
| Tracking $p/\theta$ resolution | 0.5 |
| Nuclear interaction | 0.4 |
| Sum in quadrature | 0.8 |

**Table 6**. Detector-related uncertainties in $\mathcal{B}(J/\psi \to \rho\pi)$.

### 4.4 Physical background

The main background contributions are summarized in table 1. The contribution of other background processes such as $\rho\eta$, $\rho\eta'$, $\phi\eta$, $\omega\eta$, $\omega\pi^0$, which are not accounted into the fit was estimated to be below 0.1% by the Monte-Carlo simulation. Thus, we get the total uncertainty due to background processes estimated of about 0.2%.

### 4.5 Detector-related uncertainties

The track reconstruction efficiency was studied by $J/\psi \to \rho^+\pi^-$ and $J/\psi \to \rho^-\pi^+$ events with reconstructed $\rho$ meson. About $7.3 \cdot 10^3$ events were selected. In $1.11 \pm 0.12\%$ of cases, the track corresponding to the charged $\pi$ meson was missed. According to the simulation, the fraction of such events was $0.53 \pm 0.01\%$, that corresponds to the difference 0.58% of the track reconstruction efficiencies. The change of this value does not exceed 0.22% with a significant tightening of the conditions on the $\rho$ meson invariant mass. That allow us to introduce correction $+1.16 \pm 0.24 \pm 0.44\%$ to the measured branching fraction. Considering $J/\psi \to \rho^0\pi^0$ process events with reconstructed $\rho^0$ meson, we determined the correction of $+1.02 \pm 0.12 \pm 0.18\%$ to the branching fraction due to missing $\pi^0$.

To estimate the systematic uncertainty related to the momentum and angular resolution, two methods were used to achieve agreement between the data and the MC simulation: we scale either the assumed systematic errors in x(t) or the drift chamber spatial resolution. The difference 0.5% between results obtained is taken as the systematic uncertainty estimate.

The trigger and event selection efficiencies are sensitive to the nuclear interaction of pions in the detector material. We estimated the uncertainty of 0.4% comparing the detection efficiencies for the $J/\psi \to \rho\pi$ decay obtained with the packages GHEISHA [31] and FLUKA [32] implemented in GEANT 3.21 [19].

The total correction of the measured branching fraction related to detector response is +2.2% with the uncertainty of about 0.8%. The corresponding contributions are listed in table 6.

The effect of other possible sources of the detector-related uncertainty was evaluated by varying the event selection criteria as presented in table 7. The observed variation in the number of selected events was significant, with a change in the condition for the $\chi^2_{\pi^+\pi^-\pi^0}$ criteria, it was about 10%, and in the absence of the condition $\chi^2_{\pi^+\pi^-\pi^0} < \chi^2_{K^+K^-\pi^0}$ reached 40%. The variations of result can originate from the already considered sources and statistical fluctuations, nevertheless we included them in the total uncertainty to obtain conservative error estimates.



JHEP06(2023)196

| Condition/Variable | Range variation | Variation $\mathcal{B}(J/\psi \to \rho\pi)$ in % |
|---|---|---|
| $\chi^2_{\pi^+\pi^-\pi^0}$ | $< \chi^2_{K^+K^-\pi^0}$ or no cut | 1.2 |
| $\chi^2_{\pi^+\pi^-\pi^0}$ | $< 70 \div 110$ | 0.3 |
| $E_1$ | $< 40 \div 80\,\mathrm{MeV}$ | 0.2 |
| $E_2$ | $< 140 \div 180\,\mathrm{MeV}$ | 0.1 |
| $\cos\theta_{\pi^+\pi^-}$ (for $\rho^\pm\pi^\mp$ modes) | $> -0.995 \div -0.900$ | 1.1 |
| $\cos\theta_{\pi^+\pi^-} + \cos\theta_{\pi^+\pi^0} + \cos\theta_{\pi^-\pi^0}$ | $< -1.15 \div 1.05$ | 0.7 |
| $E/p$ | $< 0.7 \div 0.8$ | 0.3 |
| $H_2/H_0$ | $< 0.75 \div 0.85$ | 0.1 |
| Sum in quadrature | | 1.8 |

**Table 7**. $\mathcal{B}(J/\psi \to \rho\pi)$ uncertainties due to variation of the selection criteria.

| Source | Uncertainty, % |
|---|---|
| Fitting model | 1.5 |
| Fitting procedure | 1.2 |
| Number of $J/\psi$ decays | 1.1 |
| Detector response | 0.8 |
| Background | 0.2 |
| Selected criteria | 1.8 |
| Sum in quadrature | 3.0 |

**Table 8**. Dominant systematic uncertainties in the $\mathcal{B}(J/\psi \to \rho\pi)$.

### 4.6 Summary of systematic uncertainties

The main sources of the systematic uncertainty on the measured branching fraction are listed in table 8.

## 5 Determination of the branching fraction of $J/\psi \to \rho(1450)\pi$ and $J/\psi \to \pi^+\pi^-\pi^0$

The fit performed in the region of invariant masses up to $1.4\,\mathrm{GeV}/c^2$, as described in section 3.2, makes it possible to determine the value of $\mathcal{B}(J/\psi \to \rho(1450)\pi)\cdot\mathcal{B}(\rho(1450) \to \pi\pi)$. However, for a more reliable determination of this value, it is necessary to expand the fitting region to $1.8\,\mathrm{GeV/c^2}$. In this case, the corresponding contributions from the $J/\psi \to \rho(1700)\pi$ and $J/\psi \to \gamma f_2$ processes must be included in the fit. These changes result in the following value $\mathcal{B}(J/\psi \to \rho(1450)\pi)\cdot\mathcal{B}(\rho(1450) \to \pi\pi) = (2.17 \pm 0.20)\cdot 10^{-4}$. The dominant systematic errors in determining the value of $\mathcal{B}(J/\psi \to \rho(1450)\pi)\cdot\mathcal{B}(\rho(1450) \to \pi\pi)$ are given in table 9.



JHEP06(2023)196

| Source | Uncertainty, % |
|---|---|
| Uncertainty $\Gamma_{\rho(1450)}$ | 9 |
| Uncertainty $M_{\rho(1450)}$ | 7 |
| Contribution $\rho(1700)\pi$ | 35 |
| Contribution $e^+e^- \to \pi^+\pi^-\pi^0$ | 33 |
| Variation of the modes separation | 15 |
| Sum in quadrature | 52 |

**Table 9**. The relative systematic uncertainties in $\mathcal{B}(J/\psi \to \rho(1450)\pi) \cdot \mathcal{B}(\rho(1450) \to \pi\pi)$.

Based on the observed number of three pion decays $J/\psi \to \pi^+\pi^-\pi^0$ over the entire range of invariant masses of pion pairs and the calculated values of the contributions $J/\psi \to \rho\pi$, $J/\psi \to \rho(1450)\pi$ and the possible contributions of the other processes, we can calculate the weighted efficiency and the quantity $\mathcal{B}(J/\psi \to \pi^+\pi^-\pi^0) = (1.841 \pm 0.013) \cdot 10^{-2}$. In a conservative approach, the systematic uncertainties of a given value included in category "Fitting model" do not exceed similar errors in table 4. Estimates of all other systematic uncertainties are the same as for the $J/\psi \to \rho\pi$ process, except for the uncertainties indicated in the 4.2 section, which, for obvious reasons, are absent. Thus, the quadratic sum of systematic uncertainties is 2.7%.

## 6 Summary

The measurement of the $J/\psi \to \rho\pi$ branching fraction is performed using the data sample of 1.4 pb$^{-1}$ collected at the $J/\psi$ resonance peak with the KEDR detector. The results are $\mathcal{B}(J/\psi \to \rho\pi) = (2.072 \pm 0.017 \pm 0.062) \cdot 10^{-2}$, $\mathcal{B}(J/\psi \to \rho(1450)\pi) \cdot \mathcal{B}(\rho(1450) \to \pi\pi) = (2.2 \pm 0.2 \pm 1.1) \cdot 10^{-4}$, and $\mathcal{B}(J/\psi \to \pi^+\pi^-\pi^0) = (1.878 \pm 0.013 \pm 0.051) \cdot 10^{-2}$ where the first uncertainty is statistical and the second one is systematic. Our results include the correction factor 1.020 due to the effects described in the sections 4.1 and 4.5. These are the most precise measurements of $\mathcal{B}(J/\psi \to \rho\pi)$ and $\mathcal{B}(J/\psi \to \pi^+\pi^-\pi^0)$ to date.

We observe substantial discrepancy with respect to the previous experiments [11–13] for the $\mathcal{B}(J/\psi \to \pi^+\pi^-\pi^0)$ value. We believe that the discrepancy with [11] are due to the fact in the present work we employ a more accurate parametrization of the $\pi - \pi$ invariant mass disribution including interference with $\rho(1450)\pi$ decay. The result [12] should be corrected taking into account changes in the measurement results of the branching fraction $\mathcal{B}(\psi(2S) \to J/\psi\pi^+\pi^-)$ which has changed by about ten percent. In addition, the method of Dalitz plot analysis of the ISR events was used in works [12, 13] and the result of our work is based on the data obtained when collecting statistics at the resonance peak.

It should be noted that in refs. [2–10], decay $\mathcal{B}(J/\psi \to \rho\pi)$ was assumed to dominate in the three-pion process, and branching $\mathcal{B}(J/\psi \to \pi^+\pi^-\pi^0)$ was actually measured. With this in mind, if we formally average the results of all experiment excluding BaBar results, we get $\mathcal{B}(J/\psi \to \pi^+\pi^-\pi^0) = (1.88 \pm 0.13) \cdot 10^{-2}$ (error includes scale factor 2.8) and this is consistent with the result of our work.



JHEP06(2023)196

We also note the result obtained for the $\mathcal{B}(J/\psi \to \rho\pi)$ branching fraction has become closer to the theoretical calculation given in [16], which, taking into account the change in experimental data, gives the value $\mathcal{B}(J/\psi \to \rho\pi) = 1.74 \cdot 10^{-2}$.


## Acknowledgments

We greatly appreciate the efforts of the staff of VEPP-4M to provide good operation of the complex during long term experiments. The authors are grateful to V.P. Druzhinin and A.I. Milstein for useful discussions. The Siberian Supercomputer Center and Novosibirsk State University Supercomputer Center are gratefully acknowledged for providing supercomputer facilities.


## A The experimental data set of the process $J/\psi \to \rho\pi$

| $M_{\pi^+\pi^-}$, GeV/c$^2$ | $n^{\rm exp}$ | $n_{\rm bkgs}$ |
|---|---|---|
| 0.324 | 1 | 0.007 |
| 0.420 | 1 | 0.061 |
| 0.444 | 3 | 0.136 |
| 0.468 | 5 | 0.154 |
| 0.492 | 3 | 0.135 |
| 0.516 | 12 | 0.269 |
| 0.540 | 22 | 0.448 |
| 0.564 | 19 | 0.719 |
| 0.588 | 37 | 0.587 |
| 0.612 | 61 | 0.908 |
| 0.636 | 83 | 1.244 |
| 0.660 | 125 | 1.993 |
| 0.684 | 247 | 2.961 |
| 0.708 | 349 | 4.131 |
| 0.732 | 464 | 6.105 |
| 0.756 | 583 | 5.061 |
| 0.780 | 616 | 1.341 |
| 0.804 | 485 | 0.711 |
| 0.828 | 437 | 0.546 |
| 0.852 | 348 | 0.531 |
| 0.876 | 262 | 0.356 |
| 0.900 | 248 | 0.273 |
| 0.924 | 178 | 0.392 |
| 0.948 | 185 | 0.281 |
| 0.972 | 145 | 0.156 |
| 0.996 | 133 | 0.159 |
| 1.020 | 122 | 0.132 |
| 1.044 | 83 | 0.067 |
| 1.068 | 76 | 0.085 |
| 1.092 | 75 | 0.255 |
| 1.116 | 63 | 0.030 |
| 1.140 | 55 | 0.292 |
| 1.164 | 58 | 0.850 |
| 1.188 | 49 | 0.011 |
| 1.212 | 39 | 0.240 |
| 1.236 | 43 | 0.004 |
| 1.260 | 31 | 0.000 |
| 1.284 | 27 | 0.009 |
| 1.308 | 23 | 0.000 |
| 1.332 | 34 | 2.275 |
| 1.356 | 14 | 0.212 |
| 1.380 | 12 | 0.005 |
| 1.404 | 13 | 0.009 |
| 1.428 | 8 | 0.014 |
| 1.452 | 7 | 0.014 |
| 1.476 | 9 | 0.006 |
| 1.500 | 9 | 0.017 |
| 1.524 | 4 | 0.011 |
| 1.572 | 2 | 0.002 |

**Table 10**. The numbers of the selected $J/\psi \to \rho^0\pi^0$ events and estimated number of the background events for the $\rho^0$ invariant mass distribution.

| | $J/\psi \to \rho^-\pi^+$ | | $J/\psi \to \rho^+\pi^-$ | |
|---|---|---|---|---|
| $M_{\pi^-\pi^0}/M_{\pi^+\pi^0}$, GeV/c$^2$ | $n^{\rm exp}$ | $n_{\rm bkgs}$ | $n^{\rm exp}$ | $n_{\rm bkgs}$ |
| 0.451 | 1 | 0 | 4 | 0.089 |
| 0.473 | 4 | 0.023 | 5 | 0.393 |
| 0.495 | 7 | 1.130 | 6 | 0.002 |
| 0.517 | 11 | 1.300 | 8 | 0.346 |
| 0.539 | 21 | 0.461 | 13 | 0.167 |
| 0.561 | 23 | 0.358 | 29 | 2.894 |
| 0.583 | 31 | 0.845 | 31 | 0.856 |
| 0.605 | 49 | 1.510 | 50 | 1.049 |
| 0.627 | 74 | 3.004 | 67 | 2.905 |
| 0.649 | 117 | 5.857 | 133 | 4.218 |
| 0.671 | 173 | 4.144 | 186 | 5.285 |
| 0.693 | 295 | 5.156 | 241 | 4.857 |
| 0.715 | 391 | 6.293 | 351 | 7.604 |
| 0.737 | 454 | 7.527 | 470 | 6.384 |
| 0.759 | 573 | 3.400 | 551 | 2.840 |
| 0.781 | 623 | 1.755 | 557 | 1.385 |
| 0.803 | 515 | 1.173 | 513 | 1.660 |
| 0.825 | 434 | 1.384 | 436 | 1.126 |
| 0.847 | 365 | 0.824 | 370 | 1.380 |
| 0.869 | 311 | 3.445 | 306 | 2.423 |
| 0.891 | 219 | 1.281 | 258 | 0.589 |
| 0.913 | 222 | 2.970 | 218 | 0.906 |
| 0.935 | 179 | 1.010 | 196 | 0.654 |
| 0.957 | 167 | 1.730 | 185 | 0.947 |
| 0.979 | 159 | 9.783 | 137 | 0.754 |
| 1.001 | 144 | 1.681 | 158 | 2.229 |
| 1.023 | 104 | 0.581 | 119 | 0.848 |
| 1.045 | 123 | 0.956 | 114 | 0.432 |
| 1.067 | 118 | 0.568 | 99 | 0.910 |
| 1.089 | 104 | 1.647 | 95 | 1.865 |
| 1.111 | 88 | 0.645 | 88 | 0.532 |
| 1.133 | 85 | 1.547 | 85 | 2.173 |
| 1.155 | 75 | 2.167 | 85 | 1.934 |
| 1.177 | 86 | 1.512 | 86 | 0.650 |
| 1.199 | 61 | 0.668 | 67 | 1.473 |
| 1.221 | 53 | 1.696 | 78 | 0.920 |
| 1.243 | 60 | 0.480 | 64 | 1.038 |
| 1.265 | 53 | 0.480 | 53 | 1.717 |
| 1.287 | 51 | 0.844 | 47 | 0.626 |
| 1.309 | 45 | 0.504 | 45 | 0.367 |
| 1.331 | 36 | 0.432 | 41 | 1.835 |
| 1.353 | 33 | 0.456 | 36 | 0.476 |
| 1.375 | 30 | 0.371 | 39 | 0.928 |
| 1.397 | 28 | 0.367 | 31 | 0.377 |
| 1.419 | 15 | 0.788 | 24 | 0.295 |
| 1.441 | 19 | 0.418 | 23 | 0.314 |
| 1.463 | 18 | 0.417 | 8 | 0.390 |
| 1.485 | 12 | 0.311 | 21 | 0.343 |
| 1.507 | 15 | 0.336 | 21 | 0.324 |
| 1.529 | 9 | 0.303 | 14 | 0.300 |
| 1.551 | 9 | 0.251 | 14 | 1.428 |
| 1.573 | 9 | 0.379 | 10 | 0.199 |
| 1.595 | 10 | 1.623 | 11 | 0.141 |
| 1.617 | 14 | 0.288 | 10 | 0.197 |
| 1.639 | 7 | 1.113 | 5 | 0.172 |
| 1.661 | 6 | 0.635 | 2 | 0.173 |
| 1.683 | 5 | 0.163 | 4 | 0.173 |
| 1.705 | 4 | 0.137 | 6 | 0.050 |
| 1.727 | 5 | 0.012 | 3 | 0.100 |
| 1.749 | 6 | 0.027 | | |
| 1.771 | 1 | 0.330 | | |

**Table 11**. The numbers of the selected $J/\psi \to \rho^-\pi^+$ and $J/\psi \to \rho^+\pi^-$ events and estimated number of the background events for the corresponding $\rho$ invariant mass distributions.

JHEP06(2023)196

## References

[1] Particle Data Group collaboration, *Review of Particle Physics*, *PTEP* **2022** (2022) 083C01 [INSPIRE].

[2] B. Jean-Marie et al., *Determination of the G Parity and Isospin of $\psi(3095)$ by Study of Multi-Pion Decays*, *Phys. Rev. Lett.* **36** (1976) 291 [INSPIRE].

[3] W. Bartel et al., *Measurement of the Branching Ratios for the Decays $J/\psi \to \rho\pi$ and $J/\psi \to \gamma\eta'$*, *Phys. Lett. B* **64** (1976) 483 [INSPIRE].

[4] DASP collaboration, *$J/\psi$ Radiative Decays Into $\pi\pi\gamma$ and $KK\gamma$*, *Phys. Lett. B* **74** (1978) 292 [INSPIRE].

[5] PLUTO collaboration, *Measurement of the $J/\psi$ Radiative Decay Into $f^0(1270)\gamma$*, *Phys. Lett. B* **72** (1978) 493 [INSPIRE].

[6] M.E.B. Franklin et al., *Measurement of $\psi(3097)$ and $\psi'(3686)$ Decays Into Selected Hadronic Modes*, *Phys. Rev. Lett.* **51** (1983) 963 [INSPIRE].

[7] MARK-III collaboration, *Measurements of $J/\psi$ Decays Into a Vector and a Pseudoscalar Meson*, *Phys. Rev. D* **38** (1988) 2695 [*Erratum ibid.* **40** (1989) 3788] [INSPIRE].

[8] BES collaboration, *Search for a vector glueball by a scan of the $J/\psi$ resonance*, *Phys. Rev. D* **54** (1996) 1221 [*Erratum ibid.* **57** (1998) 3187] [INSPIRE].

[9] BES collaboration, *Measurement of the branching fraction of $J/\psi \to \pi^+\pi^-\pi^0$*, *Phys. Rev. D* **70** (2004) 012005 [hep-ex/0402013] [INSPIRE].

[10] BaBar collaboration, *Study of $e^+e^- \to \pi^+\pi^-\pi^0$ process using initial state radiation with BaBar*, *Phys. Rev. D* **70** (2004) 072004 [hep-ex/0408078] [INSPIRE].

[11] BESIII collaboration, *Precision measurement of the branching fractions of $J/\psi \to \pi^+\pi^-\pi^0$ and $\psi' \to \pi^+\pi^-\pi^0$*, *Phys. Lett. B* **710** (2012) 594 [arXiv:1202.2048] [INSPIRE].

[12] BaBar collaboration, *The $e^+e^- \to 2(\pi^+\pi^-)\pi^0, 2(\pi^+\pi^-)\eta, K^+K^-\pi^+\pi^-\pi^0$ and $K^+K^-\pi^+\pi^-\eta$ Cross Sections Measured with Initial-State Radiation*, *Phys. Rev. D* **76** (2007) 092005 [*Erratum ibid.* **77** (2008) 119902] [arXiv:0708.2461] [INSPIRE].

[13] BABAR and BaBar collaborations, *Study of the process $e^+e^- \to \pi^+\pi^-\pi^0$ using initial state radiation with BABAR*, *Phys. Rev. D* **104** (2021) 112003 [arXiv:2110.00520] [INSPIRE].

[14] H.-Y. Cheng, C.-W. Chiang and C.-K. Chua, *Width effects in resonant three-body decays: B decay as an example*, *Phys. Lett. B* **813** (2021) 136058 [arXiv:2011.03201] [INSPIRE].

[15] D. Stamen et al., *Analysis of rescattering effects in $3\pi$ final states*, *Eur. Phys. J. C* **83** (2023) 510 [arXiv:2212.11767] [INSPIRE].

[16] F.V. Flores-Baez, *Towards an effective description for the $J/\psi$ decays*, *J. Phys. Conf. Ser.* **761** (2016) 012084 [INSPIRE].

[17] G.J. Gounaris and J.J. Sakurai, *Finite width corrections to the vector meson dominance prediction for $\rho \to e^+e^-$*, *Phys. Rev. Lett.* **21** (1968) 244 [INSPIRE].



JHEP06(2023)196

[18] N.N. Achasov et al., *A fresh look at $\phi$-$\omega$ mixing*, *Int. J. Mod. Phys. A* **7** (1992) 3187 [*Sov. J. Nucl. Phys.* **54** (1991) 664] [*Yad. Fiz.* **54** (1991) 1097] [INSPIRE].

[19] R. Brun et al., *Detector Description and Simulation Tool*, CERN Program Library Long Writeup W5013 (1994).

[20] J.C. Chen et al., *Event generator for $J/\psi$ and $\psi(2S)$ decay*, *Phys. Rev. D* **62** (2000) 034003 [INSPIRE].

[21] T. Sjostrand and M. Bengtsson, *The Lund Monte Carlo for jet fragmentation and $e^+e^-$ physics — jetset version 6.3 — an update*, *Comput. Phys. Commun.* **43** (1987) 367 [INSPIRE].

[22] KEDR collaboration, *Measurement of $\Gamma_{ee}(J/\psi)$ with KEDR detector*, *JHEP* **05** (2018) 119 [*Addendum ibid.* **07** (2020) 112] [arXiv:1801.01958] [INSPIRE].

[23] S. Jadach, W. Placzek and B.F.L. Ward, *BHWIDE 1.00: $\mathcal{O}(\alpha)$ YFS exponentiated Monte Carlo for Bhabha scattering at wide angles for LEP1/SLC and LEP2*, *Phys. Lett. B* **390** (1997) 298 [hep-ph/9608412] [INSPIRE].

[24] A.B. Arbuzov et al., *Monte-Carlo generator for $e^+e^-$ annihilation into lepton and hadron pairs with precise radiative corrections*, *Eur. Phys. J. C* **46** (2006) 689 [hep-ph/0504233] [INSPIRE].

[25] V.V. Anashin et al., *The KEDR detector*, *Phys. Part. Nucl.* **44** (2013) 657 [INSPIRE].

[26] V. Anashin et al., *VEPP-4M collider: Status and plans*, in the proceedings of the *6th European Particle Accelerator Conference (EPAC 98)*, S. Myers, L. Liijeby, C. Petit-Jean-Genaz, J. Poole and K.-G. Rensfelt eds., Stockholm, Sweden, 22–26 June 1998, IOP Publishing, Philadelphia U.S.A. (1998), p. 400–402 [INSPIRE].

[27] K.Yu. Todyshev, *On the question of the analysis of $J/\psi \to \rho\pi \to \pi^+\pi^-\pi^0$*, *LHEP* **2022** (2022) 329 [arXiv:2208.13517] [INSPIRE].

[28] G.C. Fox and S. Wolfram, *Event Shapes in e+ e- Annihilation*, *Nucl. Phys. B* **149** (1979) 413 [*Erratum ibid.* **157** (1979) 543] [INSPIRE].

[29] SND collaboration, *Study of dynamics of the process $e^+e^- \to \pi^+\pi^-\pi^0$ in the energy range 1.15–2.00 GeV*, *Eur. Phys. J. C* **80** (2020) 993 [arXiv:2007.14595] [INSPIRE].

[30] BaBar collaboration, *Dalitz plot analyses of $J/\psi \to \pi^+\pi^-\pi^0$, $J/\psi \to K^+K^-\pi^0$, and $J/\psi \to K^0_S K^\pm\pi^\mp$ produced via $e^+e^-$ annihilation with initial-state radiation*, *Phys. Rev. D* **95** (2017) 072007 [arXiv:1702.01551] [INSPIRE].

[31] H.S. Fesefeldt, *The simulation of hadronic showers: physics and applications*, PITHA-85-02, III Physilakisches Institut, RWTH Aachen Physikzentrum, 5100 Aachen, Germany (1985).

[32] A. Fasso et al., *The FLUKA code: Present applications and future developments*, *eConf* **C0303241** (2003) MOMT004 [physics/0306162] [INSPIRE].

JHEP06(2023)196